View metadata, citation and similar papers at core.ac.uk

brought to you by CORE

provided by Elsevier - Publisher Connector

Specific Binding of Ethanol to Cholesterol in Organic Solvents

Vladimir A. Daragan,* Alexei M. Voloshin,* Svetlana V. Chochina,† Teodor N. Khazanovich,‡ W. Gibson Wood,† Nicolai A. Avdulov,† and Kevin H. Mayo*

*Department of Biochemistry, Molecular Biology and Biophysics, University of Minnesota Health Sciences Center, Minneapolis, 55455, and †VA Medical Center, GRECC, and Department of Pharmacology, University of Minnesota, Minneapolis, Minnesota 55417, and ‡Institute of Chemical Physics, Russian Academy of Science, Moscow 117977, Russia

ABSTRACT Although ethanol has been reported to affect cholesterol homeostasis in biological membranes, the molecular mechanism of action is unknown. Here, nuclear magnetic resonance (NMR) spectroscopic techniques have been used to investigate possible direct interactions between ethanol and cholesterol in various low dielectric solvents (acetone, methanol, isopropanol, DMF, DMSO, chloroform, and CCl_4). Measurement of ^{13}C chemical shifts, spin-lattice and multiplet relaxation times, as well as self-diffusion coefficients, indicates that ethanol interacts weakly, yet specifically, with the HC-OH moiety and the two flanking methylenes in the cyclohexanol ring of cholesterol. This interaction is most strong in the least polar-solvent carbon tetrachloride where the ethanol–cholesterol equilibrium dissociation constant is estimated to be 2×10^{-3} M. ^{13}C-NMR spin-lattice relaxation studies allow insight into the geometry of this complex, which is best modeled with the methyl group of ethanol sandwiched between the two methylenes in the cyclohexanol ring and the hydroxyl group of ethanol hydrogen bonded to the hydroxyl group of cholesterol.

INTRODUCTION

Although some effects of ethanol on the lipid bilayers of model and biological membranes have been documented (Seeman, 1972; Chin and Goldstein, 1977), they are not well understood. It is generally accepted that ethanol interacts with both membrane proteins and membrane lipids. Accounting for up to 42 mol% of total plasma membrane lipid, cholesterol, whose chemical structure is illustrated in Fig. 1, is one of the major lipids within the plasma membrane (Wood et al., 1990). In general, cholesterol is distributed nonuniformly in the membrane. For example, in synaptic plasma membranes, about 88% of total cholesterol is localized within the cytofacial leaflet, with the remaining 12 mol% being found within the exofacial leaflet (Wood et al., 1990). In the membrane, cholesterol has multiple functions that include regulation of antioxidant action and membrane fluidity.

Like cholesterol, ethanol is also nonuniformly distributed within the membrane, being partitioned into the hydrophobic core of the lipid bilayer, which is a highly hydrophobic environment having a dielectric constant in the range of 2 to 3 (Colles et al., 1995). Due in part to this partitioning, ethanol affects cholesterol homeostasis in biological membranes and, as with cholesterol, is known to modify membrane fluidity in a nonhomogeneous or asymmetric fashion. Ethanol-induced changes in membrane fluidity have been observed using electronic paramagnetic resonance spectroscopy with spin-labeled membrane components (Chin and Goldstein, 1977) and fluorescence spectroscopy with a variety of fluorescent probes including 1,6-diphenyl-1,3,5-hexatriene (Nambi et al., 1988) and pyrene (Avdulov et al., 1994). The effect of ethanol on membrane fluidity, however, is probably underestimated because of its partitioning into the hydrophobic core of the lipid bilayer (Colles et al., 1995). The exofacial leaflet in ethanol-treated mice has been found to be significantly less fluid than the exofacial leaflet in pair-fed controls (Wood et al., 1989). Chronic ethanol consumption also alters transbilayer cholesterol distribution in synaptic plasma membranes. The synaptic plasma membrane exofacial leaflet of an ethanol-tolerant group of mice contained twice as much cholesterol compared to the exofacial leaflet of pair-fed controls (Wood et al., 1990). This observation is in agreement with the effects of ethanol treatment on the fluidity in vertical domains. Effects of chronic ethanol consumption on exchangable and nonexchangable pools of cholesterol have also been reported (Wood et al., 1993). The rate of cholesterol exchange is significantly slower in synaptosomes of ethanol-treated mice compared to their pair-fed controls (Wood et al., 1993).

Although the effects of ethanol on cholesterol dynamics in membranes are well documented (Rigby et al., 1996; Barry and Gawrich, 1995; Mitchell and Litman, 1994), the molecular mechanism of action remains unknown. Based primarily on these previous studies, we postulated that ethanol interacts directly with cholesterol. In fact, direct displacement of cholesterol from its binding sites on lipid carrier proteins SCP-2 and bovine serum albumin by ethanol has been demonstrated (Avdulov et al., 1996, 1999). The present nuclear magnetic resonance (NMR) spectroscopic study was designed to test the hypothesis that ethanol interacts with cholesterol. Although a more biologically relevant study of ethanol binding to cholesterol would be

Received for publication 6 July 1999 and in final form 14 April 2000.

Address reprint requests to Dr. Kevin H. Mayo, University of Minnesota Health Sciences Center, Dept. of Biochemistry, 6-155 Jackson Hall, 321 Church Street, Minneapolis, MN 55455. Tel.: 612-625-9968; Fax: 612-624-5121; E-mail: mayox001@maroon.tc.umn.edu.

© 2000 by the Biophysical Society

0006-3495/00/07/406/10 $2.00

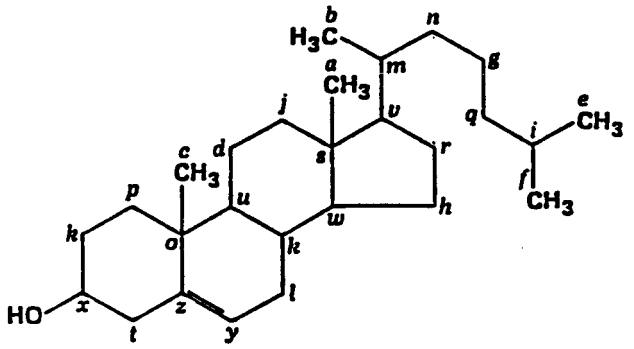

FIGURE 1 Planar representation of the chemical structure of cholesterol. Carbon atoms are labeled with lower case letters.

undertaken in vivo or in vitro using, for example, blood plasma, neat nonpolar organic solutions covering a range of low dielectrics (acetone, methanol, isopropanol, carbon tetrachloride, dimethyl formamide, dimethylsulfoxide, and chloroform) were used to simplify data interpretation and yet to mimic the hydrophobic environment within a membrane where ethanol resides within the lipid bilayer. Potential cholesterol–ethanol complex formation should be reflected in various NMR parameters: ^{13}C chemical shifts, spin-lattice relaxation rates, self-diffusion coefficients, paramagnetic-induced relaxation effects, cross-correlation spectral densities derived from ^{13}C multiplet relaxation, and theoretical calculations. The anisotropy of rotational motions of these molecules in solution will be different in the free and bound states, and the larger mass and volume of the cholesterol–ethanol complex should be reflected in changes in translational and rotational diffusion. Moreover, insight into the molecular geometry of the complex can be derived by using intermolecular relaxation rates. NMR and modeling data demonstrate formation of a weak, yet specific, complex between ethanol and cholesterol, especially strong in the most nonpolar solvent carbon tetrachloride.

MATERIALS AND METHODS

Samples enriched with ^{13}C (3,4-$^{13}C_2$, 99% cholesterol and 1,2-$^{13}C_2$, 99% ethanol) were purchased from Cambridge Isotope Laboratories, Inc. (Cambridge, MA). NMR data were acquired on Bruker AM-250 and on Varian Inova Unity Plus-500 NMR spectrometers operating at ^{13}C frequencies of 62.5 MHz and 125 MHz, respectively. The temperature was varied from 278 K to 313 K after calibration using the chemical shifts from the internal standard methanol. The following subsections describe the specific NMR experiments that were performed: ^{13}C-relaxation (T_1 [auto- and cross-correlation] and nuclear Overhauser effect (NOE)), and pulsed field gradient (PFG) self-diffusion. In addition, the rotational diffusion tensor for cholesterol was calculated using Kirkwood–Steel–Huntress theory.

NMR relaxation measurements

Spin-lattice relaxation rates were determined by using the homonuclear inversion-recovery method with the relaxation delay set at greater than 5 × T_1. The number of acquisitions was chosen to give a signal-to-noise ratio greater than 6. Ten to fifteen time-incremented (partially relaxed) spectra were routinely acquired for each relaxation measurement. To reduce errors arising from radio-frequency field inhomogeneities, a composite 180° pulse [$90°_x - 180°_y - 90°_x$] was used. To reduce contributions from nonexponential relaxation, initial relaxation rates were determined as described by Daragan et al. (1993). ^{13}C-{^1H} NOE coefficients were measured by using a standard gated decoupling technique; NOE values fell close to their maximum theoretical limit, indicating that the extreme narrowing approximation can be used to calculate rotational correlation times.

Cross-correlation times $\tau_{HCH} = \tau_{CH,CH'}$ for methyl and methylene groups were determined from proton-coupled ^{13}C relaxation data (Werbelow and Grant, 1977; Daragan and Mayo, 1997). Correlation times for motions of CH and CH′ bonds, $\tau_{CH,CH'}$, are defined as

$$\tau_{CH,CH'} = 4\pi \int_0^\infty \langle Y_{20}(\theta_{CH}(t) Y_{20} * (\theta_{CH'}(0)\rangle \, dt \qquad (1)$$

where Y_{20} is the second-order spherical harmonic, and $\theta_{CH}(t)$ is the angle between the CH-bond and the Z-axis in the laboratory frame. When CH = CH′, $\tau_{CH,CH} = \tau_{CH}$ is referred to as the autocorrelation time. For CH_2- and CH_3-groups, cross-correlation times (CH ≠ CH′), τ_{HCH}, are proportional to the difference of the initial relaxation rates of outer W_o and inner W_i lines of the ^{13}C multiplet spectrum:

$$\tau_{HCH} = \frac{4\pi^2 (W_o - W_i) r_{CH}^6}{\nu h^2 \gamma_C^2 \gamma_H^2}. \qquad (2)$$

For CH_2-groups, the coefficient $\nu = 6/5$, whereas for CH_3-groups, $\nu = 12/5$. γ_C and γ_H are the gyromagnetic ratios for carbon and proton, respectively, and h is Planck's constant. r_{CH} is the length of CH-bond taken to be 1.09 Å. Initial relaxation rates for outer and inner lines of ^{13}C multiplets, W_o and W_i, are average values of the respective relaxation rates for left and right lines of the multiplet. For example, the relaxation rate for outer lines is

$$W_o = \tfrac{1}{2}(W_o^{left} + W_o^{right}). \qquad (3)$$

A similar expression can be written for inner lines of the methyl quartet. This averaging allows elimination of cross-correlations between dipolar and chemical shift anisotropy (Bain and Linden-Bell, 1975; Daragan and Mayo, 1993). Autocorrelation times, τ_{CH}, for CH-bond rotations have been determined from proton-decoupled ^{13}C relaxation rates, W_C,

$$\tau_{CH} = \frac{4\pi^2 W_C r_{CH}^6}{N_p h^2 \gamma_C^2 \gamma_H^2}, \qquad (4)$$

where N_p is the number of protons attached to a particular carbon atom.

Rotational diffusion tensor calculations

To calculate the rotational diffusion tensor, the modified Kirkwood–Steel–Huntress theory was used (Daragan and Mayo, 1997; Steele, 1963; Huntress, 1970; Gladkii et al., 1987). This theory relates components of the rotational diffusion tensor: D_{xx}, D_{yy}, D_{zz}, to second derivatives of the intermolecular potential. Using the Langevin equation for rotational motion, the D_{xx} component of the rotational diffusion tensor can be written as (Steele, 1963; Huntress, 1970)

$$D_{xx} = k_B T \sqrt{\frac{\pi}{2 I_{xx}}} \left\langle \frac{\partial^2 U}{\partial \theta_x^2} \right\rangle^{-(1/2)}. \qquad (5)$$

I_{xx} is the molecular moment of inertia relative to the X-axis; θ_x is the angle of rotation about the X-axis; U is the potential for interactions between solute and solvent molecules; k_B is the Boltzman constant, and the angular bracket denotes an ensemble average. The potential U is considered to be the sum of atom–atom interactions. By approximating solvent molecules as spheres and assuming a Lennard–Jones type potential for interactions between atom k and a solvent molecule s, one can write

$$U = \sum_{k,s} U_{ks}(r_{ks}) = 4\varepsilon_{ks} \sum_{k,s} [(\sigma_{ks}/r_{ks})^6 - (\sigma_{ks}/r_{ks})^{12}], \quad (6)$$

where ε_{ks} and σ_{ks} are parameters of the Lennard–Jones potential. ε_{ks} is equal to the depth of the potential well, and σ_{ks} is a distance close to the minimum of this potential.

Translational self-diffusion coefficients were also calculated using the Kirkwood theory (see, for example, Naghzaden and Rice, 1962 and Daragan and Ilyina, 1987) where the self-diffusion coefficient is given by:

$$D_t = k_B T \sqrt{\frac{3\pi}{2m}} (\langle \partial^2 U/\partial R^2 \rangle)^{-(1/2)}. \quad (7)$$

m is the molecular mass, and $\langle \partial^2 U/\partial R^2 \rangle$ is the average of second derivative of the intermolecular displacement potential, which can be calculated as the average,

$$\left\langle \frac{\partial^2 U}{\partial R^2} \right\rangle = \frac{1}{3}\left(\left\langle \frac{\partial^2 U}{\partial x^2} \right\rangle + \left\langle \frac{\partial^2 U}{\partial y^2} \right\rangle + \left\langle \frac{\partial^2 U}{\partial z^2} \right\rangle \right). \quad (8)$$

x, y, z are coordinates for the center of inertia of the molecule in the laboratory frame.

The molecular geometry of the ethanol–cholesterol complex was calculated on a Silicon Graphics Indigo II workstation using the program DISCOVER (Version 3.1 Biosym Technologies, San Diego, CA) with AMBER potential energy parameters. An ethanol molecule was manually docked to a cholesterol molecule (1:1 complex) in two different orientations as discussed in the text, and energy minimization was performed on the complex. Components of the rotational diffusion tensor and self-diffusion coefficients were then calculated using the program TENSOR-2 developed by Daragan and Mayo (1997). Lennard–Jones atom–atom potentials were taken from (Eliel et al., 1965) because it was shown (Gladkii et al., 1987) that the ratio of rotational diffusion tensor components is insensitive to the potential used.

Self-diffusion measurements

Translational self-diffusion coefficients were measured using PFG NMR with a 5-mm triple-resonance probe equipped with an actively shielded z-gradient coil. The linearity of the gradient was checked by performing diffusion measurements on water over different ranges of the gradient. The PFG longitudinal eddy-current delay pulse sequence (Gibbs and Johnson, 1991) was used for all self-diffusion measurements. Each diffusion constant was determined from a series of 15–20 one-dimensional spectra acquired using different gradient strengths as described by Mayo et al. (1996).

By measuring the translational diffusion coefficients for ethanol, cholesterol, and for a 1:1 molar mixture of both, the diffusion coefficient for the cholesterol–ethanol complex can be estimated using the following procedure. With ζ being the fraction of molecules bound (which is the same for ethanol and for cholesterol in a 1:1 molar mixture), one can write

$$D^{exp}_{chol} = D^{free}_{chol}\,\xi + (1 - \xi)D^{complex}, \quad (9a)$$

$$D^{exp}_{ethanol} = D^{free}_{ethanol}\,\xi + (1 - \xi)D^{complex}, \quad (9b)$$

where D^{exp} are experimental values of the self-diffusion coefficient in the cholesterol–ethanol mixture; D^{free} are self-diffusion coefficients for ethanol or cholesterol, and $D^{complex}$ is the self-diffusion coefficient for the ethanol–cholesterol complex.

For the equilibrium between free ethanol (E) and cholesterol (C) and a 1:1 complex (EC),

$$E + C \rightleftharpoons EC, \quad (10)$$

the association equilibrium constant,

$$K_a = \frac{[EC]}{[E][C]}, \quad (11)$$

was derived by analyzing the concentration-dependent change in the chemical shift of cholesterol resonances. In general, using any NMR parameter P, one can write

$$P = pP_{complex} + (1 - p)P_{free}, \quad (12)$$

where p is the fraction of molecules in the complex, and P_{free} and $P_{complex}$ are NMR parameters (chemical shift change, $\Delta\delta$, in this case) that correspond to molecules in free and complexed states, respectively. Because the ethanol concentration had to remain less than 30 millimolar to avoid self-association and cholesterol solubility varied with the composition of the solution, NMR chemical-shift data were acquired at various molar ratios of [cholesterol]/[ethanol] and plotted as the chemical shift change, $\Delta\delta$, in ppm vs. [cholesterol]/[ethanol] for the carbons of methylene and methyl groups of ethanol and for the carbons k, t, and x of cholesterol (see Fig. 1). These plots were fit by minimizing the function $\chi^2 = \Sigma_i (\Delta\delta_i^{exp} - \Delta\delta_i^{calc})^2$ where $\Delta\delta^{exp}$ and $\Delta\delta^{calc}$ are experimental and calculated chemical-shift changes defined by P in Eq. 12. The actual concentrations of ethanol and cholesterol, and not the ratio [cholesterol]/[ethanol] itself, was used. Because K_a has the same value over the entire curve, derived populations for free and complexed states were used to calculate values for K_a according to Eq. 11. K_a values were the same for chemical shift changes of all carbons analyzed, ethanol and cholesterol.

RESULTS

Because ethanol is known to self-associate, especially in low dielectric solvents (Emsley et al., 1965) like those used in this study, the aggregation potential of ethanol in each solvent (acetone, methanol, isopropanol, CCl_4, DMF, DMSO, and chloroform) was assessed by following the ^{13}C chemical shifts of ethanol carbon resonances as a function of the ethanol concentration (data not shown). For example, below 0.1 M ethanol in CCl_4, the chemical shift of the ethanolic methyl resonance remains relatively constant, indicating the absence of ethanol self-association. To be confident that ethanol remains monomeric within this concentration range, NMR PFG self-diffusion measurements were performed with the resulting translational diffusion constant, D, of 30×10^{-7} cm^2/s at 5°C, consistent with ethanol being monomeric below 0.1 M (data not shown). For assurance that cholesterol itself does not self-associate under experimental conditions used in this study, similar controls were performed with cholesterol in each of these solvents. Because, at higher concentration, cholesterol is known to form micelles, the critical micelle concentration (CMC) for

cholesterol in the various solvents was determined by measuring light scattering as a function of the cholesterol concentration from 1 to 20 mg/ml. CMC values were calculated from the X-intercept of a linear regression line (plotted as log [cholesterol concentration] vs. light scattered) for concentrations of cholesterol where a rapid increase in light scattering was observed. In CCl_4, for example, cholesterol has a CMC of 11.3 ± 1.1 mg/ml; therefore, the cholesterol concentration in this solvent was adjusted to remain well below its CMC.

The chemical shifts of ^{13}C-resonances (methyl and methylene) in ethanol are plotted as a function of the cholesterol:ethanol molar ratio in Fig. 2. For this experiment, cholesterol was dissolved in CCl_4. Because ethanol self-associates above ~30 mM and the cholesterol solution became cloudy at some concentrations, it was not possible to perform a normal titration where the concentration of one compound was held constant as the other was varied. Therefore, the cholesterol:ethanol ratio was adjusted to avoid these problems, and changes in chemical shift reported in Fig. 2 are plotted with respect to the cholesterol:ethanol ratio. Ethanol and cholesterol concentrations ranged from 0.01 M to 0.03 M and from 0.02 M to 0.0075 M, respectively. ^{13}C chemical-shift differences ($\Delta\delta$) were calculated by subtracting the ^{13}C chemical shift of a resonance from ethanol dissolved in pure CCl_4 from that same resonance of ethanol dissolved in CCl_4 and in the presence of cholesterol. Chemical-shift changes in cholesterol were also followed (data not shown) and show similar trends. In this format (Fig. 2), these data were fitted directly using the Monte-Carlo minimization protocol described in the Methods Section. Qualitatively, however, ethanol and cholesterol must be interacting because the chemical shifts of both ethanol and cholesterol vary significantly as the cholesterol:ethanol molar ratio is changed. Furthermore, because the mid-point of these curves occurs at a cholesterol:ethanol ratio of ~1, the binding stoichiometry is probably 1:1. Similar measurements were performed using the other solvents: acetone, methanol, isopropanol, DMF, DMSO, and chloroform, and, although chemical shifts did vary, changes were usually not as large as with CCl_4. The one exception was chloroform where the maximum chemical shift difference was 0.04 ppm as opposed to 0.08 in CCl_4.

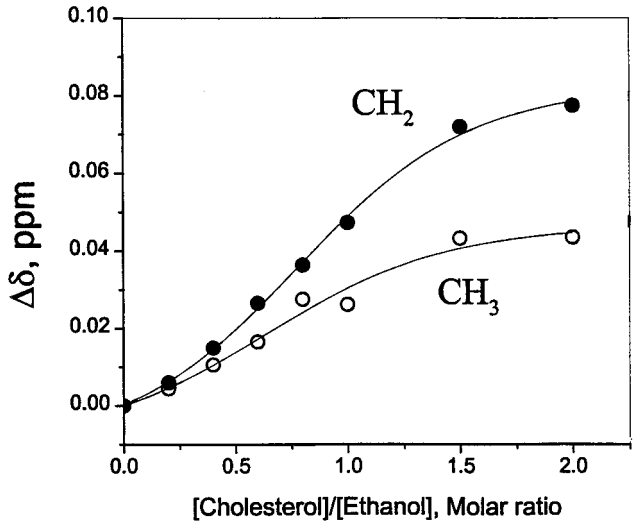

FIGURE 2 Relative ^{13}C chemical shift of the ethanol methyl carbon is plotted as a function of the cholesterol:ethanol molar ratio. NMR data were accumulated at 5°C. ^{13}C chemical shifts shown are calculated as the difference ($\Delta\delta$) between carbon chemical shifts of pure ethanol in CCl_4 from those of ethanol in the cholesterol:ethanol mixture in CCl_4.

To quantify the interaction of ethanol with cholesterol, association equilibrium constants, K_a, were calculated as described in the Methods Section. Since ethanol and cholesterol were found not to self-associate under conditions of these experiments, the analysis was simplified. Using Monte-Carlo minimization, NMR chemical shift data (Fig. 2) were fit with Eqs. 11 and 12 to derive K_a. The average K_a value is 120 ± 30 M^{-1}. A similar value for K_a was derived using the fraction bound from the diffusion data discussed above.

For further insight into ethanol–cholesterol binding, translational diffusion coefficients, D_t, were determined for cholesterol and ethanol in CCl_4. At 5°C, D_t for ethanol alone in CCl_4 is 1.96×10^{-5} cm^2/s, and D_t for cholesterol alone in CCl_4 is 0.8×10^{-5} cm^2/s. For a 1:1 molar ratio of cholesterol–ethanol in CCl_4, $D_t = 1.46 \times 10^{-5}$ for ethanol and $D_t = 0.78 \times 10^{-5}$ cm^2/s for cholesterol. Using these data and Eq. 9, the diffusion coefficient for the complex was calculated to be 0.74×10^{-5} cm^2/c, which is 8% less than that for cholesterol alone in CCl_4. Theoretically, using self-diffusion coefficients calculated by Eq. 7 and considering the intermolecular potential as a sum of atom–atom Lennard–Jones potentials (Daragan and Ilyina, 1987), a 1:1 cholesterol–ethanol complex should have a self-diffusion coefficient 13% less than that for pure cholesterol. This theoretical value agrees relatively well with the experimentally determined value, consistent with a 1:1 binding stoichiometry.

Because NMR relaxation data are more sensitive to complex formation than are chemical shift differences, ^{13}C-relaxation rates for CH_2- and CH_3-groups of ethanol in each of these solvents were measured in the presence and absence of cholesterol (1:1 molar ratio with ethanol). Typical relaxation data are exemplified in Fig. 3 for solvents CCl_4 and DMF as a function of temperature. In DMF, even at low temperature, there is little effect on the relaxation rates of carbons in ethanol in the presence of cholesterol. This is consistent with chemical-shift data. In CCl_4, however, the effect was quite large. At low temperature in CCl_4, addition of cholesterol increases ^{13}C relaxation rates almost fourfold. Such differences among solvents suggest that a particular solvent molecule can compete with ethanol for interaction with cholesterol. The relative effect from chemical shift

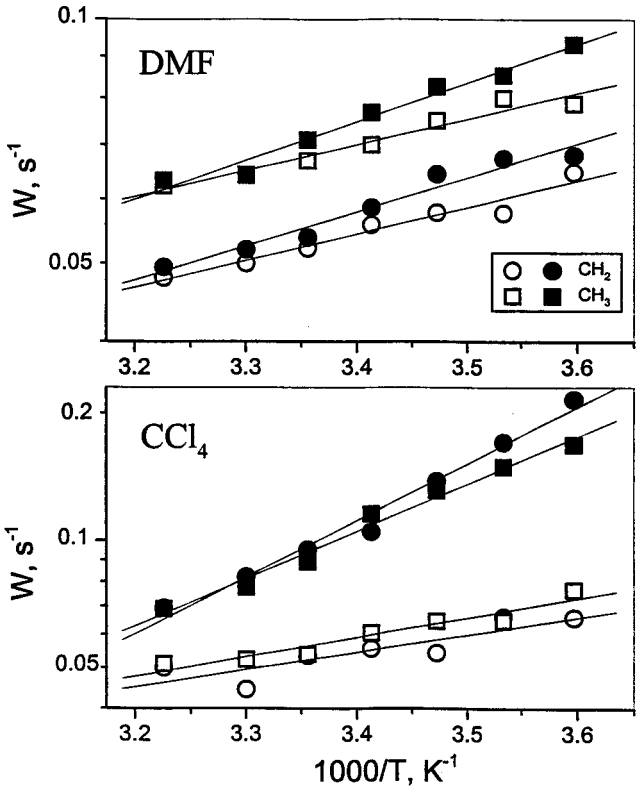

FIGURE 3 The temperature dependence of ^{13}C NMR relaxation rates of methylene (*squares*) and methyl (*circles*) groups of ethanol in DMF (*top*) and in CCl_4 (*bottom*), with (*filled symbols*) and without (*open symbols*) cholesterol. The cholesterol/ethanol molar ratio was 1:1.

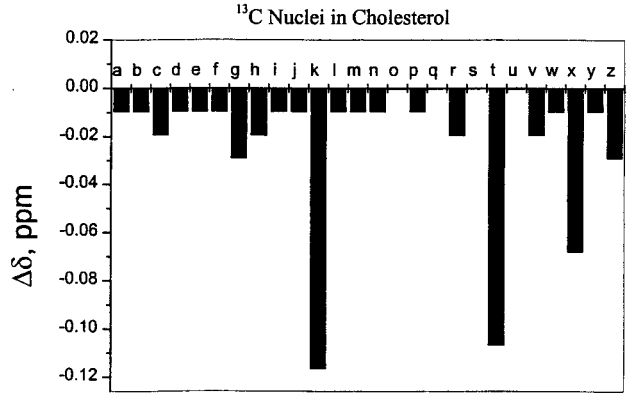

FIGURE 4 ^{13}C chemical shift difference ($\Delta\delta$) between pure cholesterol in carbontetrachloride and cholesterol a 1:1 mixture of cholesterol:ethanol in carbontetrachloride. Lower case letters identify specific carbon atoms in cholesterol as labeled in Fig. 1.

differences and relaxation rates allow the following ranking of solvents to be made from best to worst: CCl_4, chloroform, DMF, DMSO, isopropanol, acetone, methanol. Furthermore, the larger effect on relaxation rates at lower temperature indicates stronger interactions, which, in turn, may suggest that binding is mediated by hydrophilic interactions, i.e., the hydroxyl group of ethanol.

Information on the specificity of the interaction between ethanol and cholesterol comes from ^{13}C chemical-shift changes of resonances in cholesterol. At a 1:1 molar ratio of cholesterol:ethanol in CCl_4, only a few cholesterol ^{13}C resonances were shifted significantly as illustrated in Fig. 4. ^{13}C resonance assignments for cholesterol were taken from Reich et al. (1969). Cholesterol resonances that shift most belong to carbons *k*, *t*, and *x*, which are all located around the hydroxyl group of the cyclohexanol ring (see Fig. 1). Aside from substantiating the observation that ethanol interacts with cholesterol, these data indicate that the interaction is specific because no other cholesterol ^{13}C resonances were similarly shifted. In chloroform, the maximum chemical-shift differences for cholesterol resonances were also observed at carbons *k* and *x*, but not at carbon *t*. This observation suggests that ethanol interacts with cholesterol in chloroform in a slightly different binding geometry than in carbon tetrachloride, but, nonetheless, at the same site on cholesterol (the C–OH region of the cyclohexanol ring). Furthermore, because the largest chemical shift and relaxation rate changes were observed in CCl_4 and in chloroform, interactions between ethanol and cholesterol are strongest in solvents having the lowest dielectrics.

Geometry of Ethanol–Cholesterol Complex

For insight into the molecular geometry of the ethanol:cholesterol complex, ^{13}C-NMR relaxation data were used to examine whether a particular structural model was consistent with the experimental data. Given that ethanol interacts specifically at the C–OH group and flanking methylenes in the cyclohexanol ring of cholesterol, two structural models (A and B) are proposed. In both, a hydrogen bond is assumed to form between the hydroxyl groups of cholesterol and ethanol, but the orientation of the ethanol molecule in each complex is different as depicted in Fig. 5. In model A, the methyl group of ethanol is sandwiched between methylenes *k* and *t*, being partially buried within the hydrophobic portion of the cyclohexanol ring, whereas in model B, the methyl group of ethanol sticks out into the solvent. Even though model B is probably less likely than model A because the methylenes flanking the C–OH group are clearly chemically shifted, model B was included as the extreme opposite case.

The ratio of ^{13}C relaxation rates, $W(CH_n)$, for any two non-coplanar ^{13}C–H vectors in a molecule is a sensitive measure of the rotational anisotropy of the molecule or of the molecular complex (Daragan and Mayo, 1997). ^{13}C-enriched cholesterol is only available for carbons enriched at positions *t* and *x* where ^{13}C–H vectors are non-coplanar. For these relaxation experiments, cholesterol was dissolved in each of the solvents used above, basically saturating cholesterol molecules with solvent molecules, and autocor-

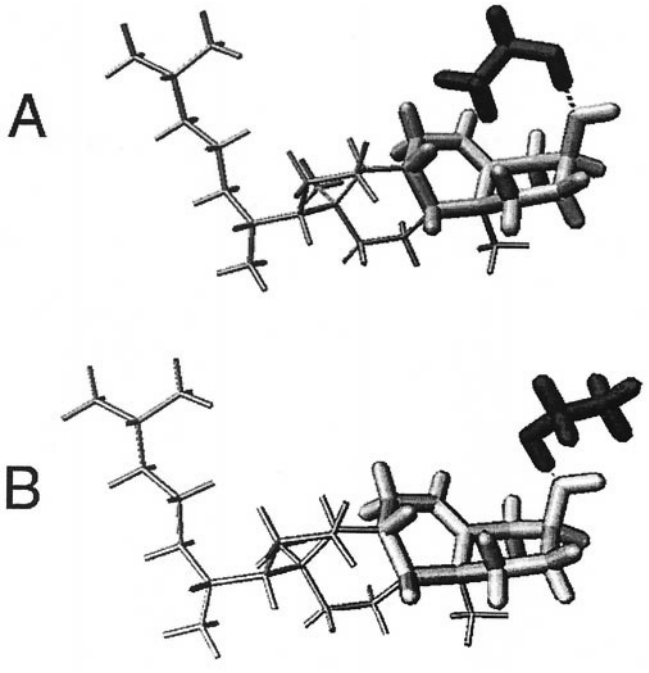

FIGURE 5 Two structural models for the cholesterol–ethanol complex. (A) The methyl group of ethanol is sandwiched between methylenes *k* and *t* and is partially buried within the hydrophobic portion of the cyclohexanol ring of cholesterol. (B) The methyl group of ethanol sticks out into the solvent. In both models, a hydrogen bond is assumed to form between the hydroxyl groups of cholesterol and ethanol. The molecule of ethanol is shaded with thicker, darker bonds. The cholesterol molecule is the other structure shown in each model, with its cyclohexanol ring highlighted with thicker bonds.

relation ^{13}CH relaxation rates were measured for both carbons *t* and *x*. The ratio of these relaxation rates, W(CH_2)/W(CH), is 1.83 ± 0.05 for all solvents (average ± SD) except for ethanol and isopropanol where the ratio drops to 1.6 ± 0.05. These data indicate that both ethanol and isopropanol, but not acetone, DMF, DMSO, CCl_4, or methanol, interact with cholesterol. Although ethanol was no surprise, results with isopropanol were unexpected because no chemical-shift changes were observed during the ethanol/cholesterol titration in isopropanol. This may be the result of efficient displacement of isopropanol in the presence of ethanol, and, in turn, may have something to do with the unique chemical properties of ethanol in that it is about half polar and half nonpolar, whereas isopropanol is more nonpolar.

Using the two structural models (A and B) for the ethanol:cholesterol complex, the rotational diffusion tensor, which is related to the ratio of relaxation rates for CH vectors *t* and *x*, was calculated using the modified Kirkwood–Steel–Huntress theory (Eq. 5) (Daragan and Mayo, 1997; Steele, 1963; Huntress, 1970; Gladkii et al., 1987). After performing averaging on Eq. 5, components of the rotational diffusion tensor were calculated for both models, as well as for cholesterol itself, using the relationship between rotational correlation times and the rotational diffusion tensor. For cholesterol alone, the calculated ratio $W(CH_2)/W(CH)$ is 1.9, which is very close to that determined experimentally (1.83). For models A and B, $W(CH_2)/W(CH)$ is calculated to be 1.3 and 1.1, respectively. For the ethanol–cholesterol mixture where the cholesterol-bound fraction is high, $W(CH_2)/W(CH)$ is experimentally found to be 1.6 ± 0.05. Inasmuch as 1.6 is closer to 1.3 than to 1.1, these data support model A.

The analysis above focused on ^{13}C relaxation rates from cholesterol. By measuring ^{13}C NMR proton-coupled relaxation rates for methyl and methylene carbons in ethanol, one can obtain four experimental parameters: two autocorrelation times, τ_{CH}, and two cross-correlation times, τ_{HCH} (Table 1). These correlation times are related to components of the rotational diffusion tensor and its orientation in the molecular frame (Avdulov et al., 1996). Here, it was assumed that anisotropic rotational diffusion of ethanol could be described by two rotational diffusion coefficients: $D_\parallel$ and $D_\perp$, i.e., symmetric top-type rotations. Z_D, which denotes the symmetry axis of the rotational diffusion tensor, lies in the C–C–O plane as illustrated in Fig. 6. The molecular coordinate system has been chosen such that the Z_M-axis of the molecular frame is directed along the O–C bond. α is the angle between Z_M and Z_D.

Using auto- and cross-correlation times given in Table 1, the orientation of the Z_D-axis was calculated (Avdulov et al., 1996) for ethanol in CCl_4 with and without cholesterol. For the cholesterol–ethanol mixture, Fig. 7 plots the calculated values of τ_{HCH}/τ_{CH} for the ethanolic methylene group as a function of the angle α and the ratio $D_\parallel/D_\perp$. This plot shows that τ_{HCH}/τ_{CH} is highly sensitive to the orientation of the main rotational axis. For ethanol in CCl_4 in the absence of cholesterol (not plotted in Fig. 7), α is equal to 4°, i.e., the main rotational axis is almost coincident with the O–C bond. In the presence of cholesterol (Fig. 7), this angle is increased to 31°, indicating a shift in the Z_D rotational axis toward the C–C bond. This effect is similar to that observed for ethanol in its interaction with the protein bovine serum albumin (Avdulov et al., 1996), where the methyl group of ethanol mediated complexation via interactions with hydro-

TABLE 1 Auto- and crosscorrelation times of the methylene and methyl groups of ethanol, τ_{CH} and τ_{HCH}, respectively, and the orientation of the *Z*-axis of the rotational diffusion tensor at 5°C in carbon tetrachloride with and without cholesterol (1:1 molar ratio)

Group	Cholesterol	τ_{CH}	τ_{HCH}
CH_2	no	1.83	0.46
CH_3	no	1.67	−0.09
CH_2	yes	8.1	5.5
CH_3	yes	4.1	−1.4

All correlation time are in ps.
The error in τ_{CH} is about 5% and the error in τ_{HCH} is about 15%.

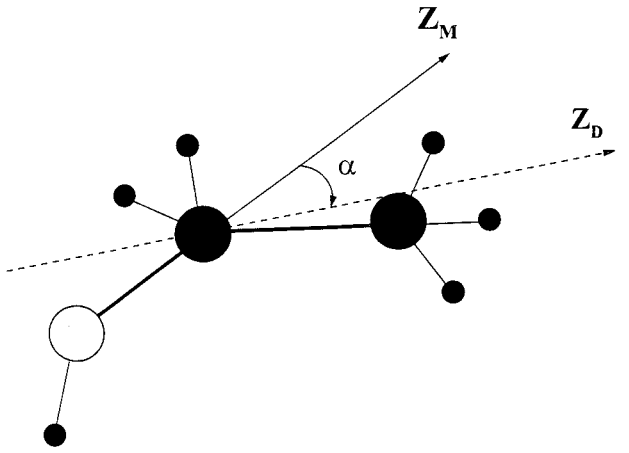

FIGURE 6 Illustration of the orientation of the *Z*-axis of the rotational diffusion tensor in ethanol. Z_D lies in the C–C–O plane and denotes the symmetry axis of the rotational diffusion tensor. The Z_M-axis of the molecular frame is directed along the O–C bond. α is the angle between Z_M and Z_D.

phobic pockets on the protein surface. In its association with cholesterol, the ethanolic methyl group interacts with methylene groups of the cyclohexanol ring. This finding supports structural model A (Fig. 5).

Additional information about the geometry of the cholesterol–ethanol complex was derived from intermolecular relaxation, which is mediated by nuclear dipole–dipole interactions among solute and solvent molecules. To assess the intermolecular contribution to relaxation rates, the paramagnetic molecule, *tris*-(acetylacetonato)$_3$ chromium (III) (Cr(acac)$_3$), was used as a relaxation agent. Chromium acetylacetonate, which is chemically inert and nonpolar, has six oxygen atoms in an octahedral array about the central

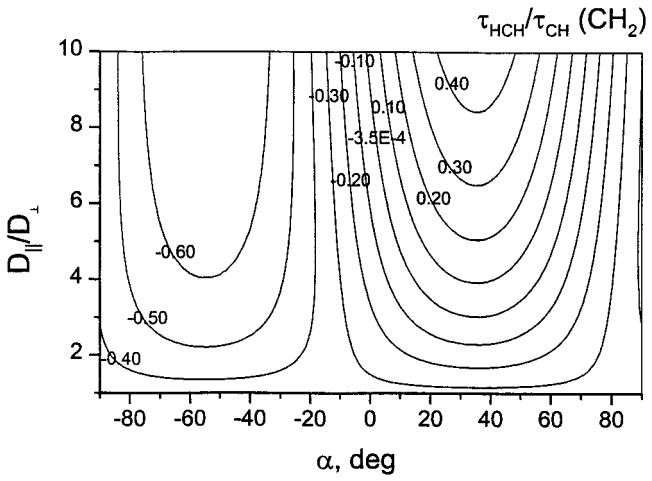

FIGURE 7 Dependence of the ratio of cross- and autocorrelation times, τ_{HCH}/τ_{CH}, for the methylene group of ethanol, on the angle α, i.e., on the orientation of the *Z*-axis of the rotational diffusion tensor and on the ratio of the components of this tensor.

metal atom with the paraffinic portion of the molecule lying on the outer surface (Hexem et al., 1976). Here, this paramagnetic agent is used to investigate changes in relaxation rates of ^{13}C nuclei of ethanol in the presence and absence of cholesterol. As a result of the unpaired electron-spin density of the metal complex, relaxation of ^{13}C nuclei will be dominated by modulation of the electron–carbon dipole–dipole interaction resulting from translational motions of ethanol and cromium acetylacetonate, rotational motions of ethanol, and internal relaxation of electron spins. This paramagnetic effect on ^{13}C relaxation rates is proportional to the concentration of the chromium acetylacetonate. Because the theory of such interactions is extremely complicated, data will be analyzed by assuming that the interactive centers of the molecules are located in the centers of spheres such that contributions to ^{13}C spin-lattice relaxation rates from electron–carbon interactions, W_e, can be expressed as (Hexem et al., 1976; Abragam, 1961; Hwang and Freed, 1975)

$$W_e \propto \gamma_C^2 \langle \mu^2 \rangle NF/Dd, \tag{13}$$

where $\langle \mu^2 \rangle$ is the mean square electron magnetic moment; N is the concentration of the paramagnetic agent; d is the distance of closest approach of the molecules, and F is a dimensionless term that contains relaxation times of electronic spins, pair correlation function of liquid molecules, and various dynamic parameters describing translational motions. D is the diffusion coefficient for relative molecular diffusion, which, in the case of independent translational motions of interacting molecules, can be expressed as the sum of individual self-diffusion coefficients for ethanol and cromium acetylacetonate,

$$D = D_{\text{ethanol}} + D_{\text{Cr(acac)}_3}. \tag{14}$$

Figure 8 plots ^{13}C relaxation rates of carbons in ethanol as a function of the concentration of cromium acetylacetonate, at two temperatures and in the absence and presence of cholesterol (1 : 1 cholesterol/ethanol molar ratio). Slopes of these curves, which reflect intermolecular interactions according to Eq. 13, are given in Table 2. Even in the absence of cholesterol, the observed trend in the relaxation data is unexpected because the intermolecular contribution to ^{13}C methylene relaxation at either temperature is greater than that to ^{13}C relaxation of the methyl group. This finding is particularly unusual because contributions to the relaxation rate from intermolecular interactions should be larger for nuclei that are further from the molecular center (Hubbard, 1963; Ayant et al., 1977; Albrand et al., 1981). The definition of molecular center for such flexible molecules as ethanol is, however, uncertain; nonetheless, in ethanol, the methyl group will always be more distant from that center than the methylene group. This contradiction may be explained by considering a local, anisotropic distribution of ethanol molecules around the cromium acetylacetonate molecule. Weak interactions between ethanol and chromium

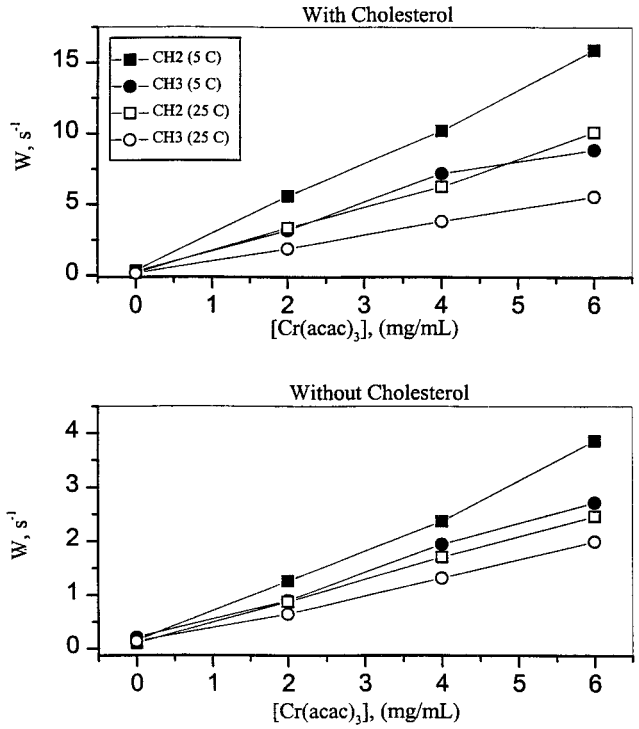

FIGURE 8 ^{13}C relaxation rates for methylene and methyl groups of ethanol as a function of the concentration of paramagnetic cromium acetylacetonate in the presence (*top*) and in the absence (*bottom*) of cholesterol. The cholesterol/ethanol molar ratio was 1:1.

acetylacetonate may promote an anisotropic distribution with the ethanolic methyl group being oriented more toward the solvent. In this instance, local anisotropy would be diminished as the temperature is increased. This is indeed the case, as can be seen by comparing data shown in Table 2 (first four rows). Another reason for differences in these slopes (Fig. 8) is that interaction with the paramagnetic center has two independent components: free relative diffusion and diffusion in a potential well $U(\rho)$ (harmonic for simplicity),

$$U(\rho) = 3k_BT\rho^2/2\langle\rho^2\rangle, \quad (15)$$

where ρ is the vector connecting the ^{13}C nucleus of a given fragment to its mean position. k_B is the Boltzman constant, and $\langle\rho^2\rangle$ is the mean square distance of ^{13}C from its mean position. Free diffusion is governed by Eq. 14, and diffusion within the harmonic potential is governed by the coefficient D_o. Assuming that the molecules are hard spheres, the spectral density function, which defines the intermolecular contribution to the relaxation rate, can be approximated by using classical relaxation theory (Abragam, 1961). For very small values of $\langle\rho^2\rangle$, i.e., for molecules without internal motions, F in Eq. 13 becomes

$$F = 8\pi/75, \quad (16)$$

and will be designated F_{rigid}. When $\langle\rho^2\rangle/d^2 \gg 1$, F_{rigid} is modulated by the two diffusion coefficients as shown in

$$F = F_{rigid}D/(D + D_o). \quad (17)$$

This relationship is valid under conditions of extreme narrowing for the nuclei and when the electron Larmor frequency falls in the region of slow motion, i.e., $\omega_e d^2/D \gg 1$. We have found that increasing $\langle\rho^2\rangle/d^2$ leads to a monotonic decrease in F from F_{rigid} to that value given by Eq. 17. For the methyl group of ethanol, the ratio $\langle\rho^2\rangle/d^2$ is greater than that for the methylene group, which can explain the trend in our experimental data.

Addition of cholesterol increases the intermolecular contribution to the relaxation rate of the ethanolic methylene group relative to the methyl group. The ratio of slopes, $(CH_2)/(CH_3)$, is increased by more than 20% at lower temperature and by more than 40% at higher temperature. These data support model A, where the ethanolic methyl group in the bound state is positioned within the hydrophobic pocket of the cyclohexanol ring of cholesterol. In this case, the distance of the methyl group from the center of the molecule is less than that for the methylene group and the intermolecular effects from the paramagnetic agent to ^{13}C methyl relaxation should be smaller. Alternatively stated, the methylene group is more exposed to the chromium acetylacetonate; therefore, its interactions with the paramagnetic center should be stronger. In this model, the internal mobility of the methyl group would be drastically reduced due to steric hinderance from groups in the cyclohexanol ring. Reduced mobility of the methyl group has been observed experimentally.

TABLE 2 Slopes of the concentration dependencies of ethanol carbon ^{13}C relaxation rates versus the concentration of *tris*-(acetylacetonato)$_3$chromium (III) with and without cholesterol (1:1 molar ratio)

Ethanol group	Temperature (°C)	Cholesterol	Slope
CH_2	5	no	0.61 ± 0.01
CH_3	5	no	0.43 ± 0.02
CH_2	25	no	0.4 ± 0.01
CH_3	25	no	0.31 ± 0.02
CH_2	5	yes	2.56 ± 0.07
CH_3	5	yes	1.49 ± 0.16
CH_2	25	yes	1.63 ± 0.07
CH_3	25	yes	0.91 ± 0.01

Slopes are given in units of $s^{-1}g^{-1}ml$.

DISCUSSION

This ^{13}C-NMR study has demonstrated that, in various organic solvents covering a range of dielectrics, ethanol interacts with cholesterol at a specific site located at the C–OH group and flanking methylenes in the cyclohexanol ring. Relaxation data and structural modeling argue that, in

this cholesterol-bound state, the ethanol molecule is oriented with its methyl group partially buried within the hydrophobic pocket of the cyclohexanol ring, with its methylene group more exposed to solvent, and with its hydroxyl group oriented toward, and possibly hydrogen-bonded to, the hydroxyl group of cholesterol. The cholesterol–ethanol interaction is strongest in solvents having the lowest dielectrics of those investigated here, i.e., carbon tetrachloride and chloroform. Although the presence of the low dielectric solvent itself might drive formation of this complex via intermolecular hydrogen bonding, the ethanolic methyl group appears to interact primarily with the hydrophobic methylene groups of cholesterol and not orient itself into the low dielectric solvent as might have been expected. Interestingly, isopropanol can also interact with cholesterol. However, because ethanol still binds to cholesterol in the presence of excess isopropanol, it appears that ethanol can readily displace isopropanol from cholesterol. Even though both alcohols contain a hydroxyl group, this may be explained, in part, by the fact that the more hydrophobic isopropanol has an additional methylene group. In the context of our model for the ethanol–cholesterol complex, isopropanol does not fit as well into the cyclohexanol ring "pocket" as does ethanol.

The question is open as to whether or not such a complex between ethanol and cholesterol could form in an actual membrane environment. In vivo, the interaction of ethanol with the cell membrane is much more complicated. In fact, the presence of ethanol within even a model membrane is an issue of considerable controversy. Most biophysical studies using model membranes indicate that ethanol interacts or binds at the lipid–water interface, with little or no ethanol residing within the hydrocarbon interior of the membrane. Direct observation of NOEs between nuclear spins of ethanol and lipid molecules in model membranes, for example, has indicated that ethanol resides with highest probability at the lipid–water interface near the lipid glycerol backbone and upper methylene segments of the lipid hydrocarbon chains (Holte and Gawrisch, 1997). In reversed lipid micelles composed of 1,2-dipalmitoyl-*sn*-glycero-3-phosphocholine (DPPC), water, and nonpolar solvent, ethanol interacts at an amphiphilic site such that the ethanol methylene is adjacent, at least in some configurations, to the methylene proximal to the carbonyl of the DPPC fatty acid moiety (Klemm and Williams, 1996).

Cholesterol, in contrast, is positioned within model membranes such that the hydrophobic steroid ring is mostly buried within the membrane and is oriented, on average, parallel to the membrane phospholipids, i.e., perpendicular to the membrane surface (Villalain, 1996). The hydroxyl group, however, is in close proximity to the phospholipid ester carbonyl groups near the solvent interface. In fact, cholesterol may even be partially solvent exposed. At least one clinical isolate of the bacterium *Pseudomonos aeruginosa* has been shown to adher to the plasma membrane of Chinese hamster ovary cells via interactions with cholesterol and cholesterol esters of the membrane (Rostand and Esko, 1993), lending support to the idea that at least part of the cholesterol molecule, possibly its cyclohexanol moiety, may be somewhat solvent exposed.

At the membrane surface, ethanol interacts with various target membrane molecules like lipids and proteins, and can compete with and displace water molecules from various sites. The basis for competition with water is the hydrogen-bonding capability of both compounds. The amphiphilic character of ethanol, however, also gives it the capability to be attracted simultaneously to both hydrophobic and hydrophilic targets of the membrane. Thus, ethanol can bind certain targets preferentially, leading to structural consequences to the membrane. Fourier transform infrared spectroscopy and NMR evidence from model membrane systems suggests that ethanol has a nonstereospecific binding capability for membrane surface molecules (Klemm, 1998). Those membrane surface molecules generally considered as targets for ethanol binding are zwitterionic phospholipids, gangliosides, and membrane proteins like glycoproteins. Given the potential for cholesterol to be at least partially solvent exposed, one addition to this list could be cholesterol, a major component of membrane lipids. In this regard, our model for the ethanol–cholesterol complex provides a reasonable model for the interaction of ethanol and cholesterol at or near the surface of a membrane.

This research was generously supported by grants from the National Institutes of Health (AA 10806) and from the North Atlantic Treaty Organization (GRG-970039). NMR experiments were performed at the University of Minnesota High Field-NMR Laboratory.

The authors are grateful to Dr. Djaudat Idiyatullin for assistance in performing the PFG self-diffusion measurements.

REFERENCES

Abragam, A. 1961. Principles of Nuclear Magnetism. Chap. 8. Oxford Univ. Press, Oxford, U.K.

Albrand, J. P., M. C. Taieb, P. Fries, and E. Belorizky. 1981. Effect of eccentricity on nuclear magnetic relaxation by intermolecular dipole–dipole interactions: ^{13}C relaxation of neopentane. *J. Chem. Phys.* 75:2141–2146.

Avdulov, N. A., S. V. Chochina, V. A. Daragan, F. Schroeder, K. H. Mayo, and W. G. Wood. 1996. Direct binding of ethanol to bovine serum albumin: a fluorescent and ^{13}C NMR multiplet relaxation study. *Biochemistry.* 35:340–347.

Avdulov, N. A., S. V. Chochina, U. Igbavboa, C. S. Warden, F. Schroeder, and W. G. Wood. 1999. Lipid binding to sterol carrier protein-2 is inhibited by ethanol. *Biochim. Biophys. Acta* 1437:37–45.

Avdulov, N. A., W. G. Wood, and R. A. Harris. 1994. Effects of ethanol on structural parameters of rat brain membranes: relationship to genetic differences in ethanol sensitivity. *Alcohol Clin. Exp. Res.* 18:53–59.

Ayant, Y., E. Belorizky, P. Fries, and J. Rosset. 1977. Intermolecular contribution to dipole–dipole relaxation rates of small molecules. *J. Physique* 38:325–337.

Bain, A. D., and R. M. Linden-Bell. 1975. The relaxation matrices for AX_2 and AX_3 nuclear spin systems. *Mol. Phys.* 30:3225–3356.

Barry, J. A., and K. Gawrich. 1995. Effects of ethanol on lipid bilayers containing cholesterol, gangliosides, and sphingomyelin. *Biochemistry.* 34:8852–8860.

Chin, J. H., and D. B. Goldstein. 1977. Effects of low concentrations of ethanol on the fluidity of spin-labeled erythrocyte and brain membranes. *Mol. Pharmacol.* 13:435–441.

Colles, S., W. G. Wood, S. C. Myers-Payne, U. Igbavboa, N. A. Avdulov, J. Joseph, and F. Schroeder. 1995. Structure and polarity of mouse brain synaptic plasma membrane: effects of ethanol in vitro and in vivo. *Biochemistry.* 34:5945–5959.

Daragan, V. A., and E. E. Ilyina. 1987. Calculation of the diffusion coefficients of polyatomic molecules in solutions. *Sov. J. Phys. Chem.* 4:654–659.

Daragan, V. A., and K. H. Mayo. 1993. Asymmetric ^{13}C NMR multiplet relaxation and dipolar-CSA cross correlation for glycine $^{13}C_{\alpha}$ methylene in peptides. *Chem. Phys. Lett.* 206:393–400.

Daragan, V. A., M. A. Kloczewiak, and K. H. Mayo. 1993. ^{13}C nuclear magnetic resonance relaxation-derived Ψ, Φ bond rotational energy barriers and rotational restrictions for glycine $^{13}C_{\alpha}$-methylene in a GXX-repeat hexadecapeptide. *Biochemistry.* 32:10580–10590.

Daragan, V. A., and K. H. Mayo. 1997. Motional model analyses of protein and peptide dynamics using ^{13}C and ^{15}N NMR relaxation. *Prog. NMR Spectrosc.* 31:63–105.

Eliel, E. L., N. L. Alliger, S. J. Angyal, and G. A. Morrison. 1965. Conformational Analysis. John Wiley & Sons, Inc., New York.

Emsley, J. W., J. Feeney, and L. H. Sutcliffe. 1965. High Resolution Nuclear Magnetic Resonance Spectroscopy, Pergamon Press, Oxford, U.K.

Gibbs, S. J., and C. S. Johnson. 1991. A PFG NMR experiments for accurate diffusion and flow studies in the presence of Eddy currents. *J. Magn. Reson.* 93:395–402.

Gladkii, A. M., V. A. Daragan, and I. V. Edneral. 1987. The calculation and ^{13}C NMR measurement of correlation times for rotational motion of mono- and disubstituted aromatic molecules in solutions. *Sov. J. Chem. Phys.* 4:825–830.

Hexem, J. G., U. Edlund, and G. C. Levy. 1976. Paramagnetic relaxation reagents as a probe for translational motion of liquids. *J. Chem. Phys.* 64:936–941.

Holte, L. L., and K. Gawrisch. 1997. Determining ethanol distribution in phospholipid multilayers with MAS-NOESY spectra. *Biochemistry.* 36: 4669–4674.

Hubbard, P. 1963. Nuclear magnetic relaxation by intermolecular dipole–dipole interactions. *Phys. Rev.* 131:275–282.

Huntress, W. T., Jr. 1970. The study of anisotropic rotation of molecules in liquids by NMR quadrupolar relaxation. *Adv. Magn. Resonance.* 4:1–28.

Hwang, L.-P., and J. H. Freed. 1975. Dynamic effects of pair correlation functions on spin relaxation by translational diffusion in liquids. *J. Chem. Phys.* 63:4017–4025.

Klemm, W. R. 1998. Biological water and its role in the effects of alcohol. *Alcohol.* 15:249–267.

Klemm, W. R., and H. J. Williams. 1996. Amphiphilic binding site of ethanol in reversed lipid micelles. *Alcohol.* 13:133–138.

Mayo, K. H., E. Ilyina, and H. Park. 1996. A recipe for designing water-soluble, β-sheet-forming peptides. *Protein Sci.* 5:1301–1315.

Mitchell, D. C., and B. J. Litman. 1994. Effect of ethanol on metarhodopsin II formation is potentiated by phospholipid polyunsaturation. *Biochemistry.* 33:12752–12756.

Naghzaden, J., and S. A. Rice. 1962. Kinetic theory of dense fluids. X. measurements and interpretation of self-diffusion in liquid Ar, Kr, Xe, and CH_4. *J. Chem. Phys.* 36:2710–2716.

Nambi, P., E. S. Rowe, and T. J. McIntosh. 1988. Studies of the ethanol-induced interdigitated gel phase in phosphatidylcholines using the fluorophore 1,6-duphenyl-1,3,5-hexatriene. *Biochemistry.* 27:9175–9182.

Reich, H. R., M. Jautelat, M. T. Messe, F. J. Weigert, and J. D. Roberts. 1969. NMR spectroscopy carbon-13 spectra of steroids. *J. Am. Chem. Soc.* 91:7445–7454.

Rigby, A. C., K. R. Barber, G. S. Shaw, and C. W. Grant. 1996. Transmembrane region of the epidermal growth factor receptor: behavior and interactions via 2H NMR. *Biochemistry.* 35:12581–12601.

Rostand, K. S., and J. D. Esko. 1993. Cholesterol and cholesterol esters: host receptors for *Pseudomonas aeruginosa* adherence. *J. Bio. Chem.* 268:24053–24059.

Seeman, P. 1972. The membrane actions of anesthetics and tranquilizers. *Pharmacol. Rev.* 24:583–655.

Steele, W. A. 1963. Molecular reorientation in liquids. I. Distribution functions and friction constants. *J. Chem. Phys.* 38:2404–2411.

Villalain, J. 1996. Location of cholesterol in model membranes by magic-angle-sample-spinning NMR. *Eur. J. Biochem.* 241:586–593.

Werbelow, L. G., and D. M. Grant. 1977. Intramolecular dipolar relaxation in multispin systems. *Adv. Magn. Resonance.* 9:189–299.

Wood, W. G., F. Schroeder, L. Hogy, A. M. Rao, and G. Nemecz. 1990. Asymmetric distribution of a fluorescent sterol in synaptic plasma membranes: effects of chronic ethanol consumption. *Biochim. Biophys. Acta.* 1025:243–246.

Wood, W. G., C. Gorka, and F. Schroeder. 1989. Acute and chronic effects of ethanol on transbilayer membrane domains. *J. Neurochem.* 52: 1925–1933.

Wood, W. G., A. M. Rao, U. Igbavboa, and M. Semotuk. 1993. Cholesterol exchange and lateral cholesterol pools in synaptosomal membranes of pair-fed control and chronic ethanol-treated mice. *Alcohol Clin. Exp. Res.* 17:345–354.